Inelastic Scattering of 20-MeV Tritons from ^{90}Zr†

E. R. FLYNN, A. G. BLAIR, AND D. D. ARMSTRONG
Los Alamos Scientific Laboratory, University of California, Los Alamos, New Mexico
(Received 26 October 1967)

The inelastic scattering of tritons from ^{90}Zr was studied at a beam energy of 20 MeV, and angular distributions of states up to 5.22 MeV of excitation were obtained. The data are compared with distorted-wave calculations, employing both collective and shell-model form factors. Both calculations reproduce the shapes of the experimental angular distributions quite well. Values of deformation parameters obtained from the collective-model form-factor calculation are in good agreement with the results of inelastic scattering experiments employing beams of ^{3}He and ^{4}He ions, but are in poor agreement with the results of proton inelastic scattering measurements. The shell-model analysis assumed an effective two-body interaction between the triton projectile and the target nucleons, and the form-factor calculation employed a Yukawa well with a 1.0-F range. Under these conditions, an effective interaction strength averaging 660 MeV was obtained for the excitation of the well-known pure proton-configuration states. This value is approximately three times the strength obtained in the previous study of proton inelastic scattering from these states. This result supports the assumption that the optical potential has a real well depth approximately three times as great for the triton as for the single nucleon. The strengths of the transitions to the other observed states are also discussed in terms of configurations expected to contribute to the states. Characteristics of the (t,t') reaction are compared with those of the (p,p') reaction.

I. INTRODUCTION

THE study of nuclear states by means of inelastic scattering of nucleons and simple composite particles has provided a large amount of spectroscopic information in recent years. Angular distributions have been used to assign spins and parities, and the strengths of the transitions have yielded information about the composition of the wave functions of the states. For the most part, these investigations have employed incident beams of protons, deuterons, and α particles. There have been fewer studies in which beams of neutrons and ^{3}He particles were used, and we are not aware of any previous studies of inelastic triton scattering.[1] Since each of these projectiles interacts somewhat differently with target nuclei, the resulting information should be somewhat different. For example, single-nucleon projectiles penetrate more deeply into the nucleus than do the other projectiles mentioned, and thus are expected to sample more of the nuclear interior than do these strongly absorbed particles. Tritons should interact somewhat differently from the other strongly absorbed particles, however, owing to their intrinsic spin of one-half and their isospin of plus one-half.

To investigate the properties of triton inelastic scattering, it seems advisable to begin by choosing a target nuclide which has previously been studied by the inelastic scattering of other projectiles, and for which the wave functions of some of the states are relatively well understood. Such a nuclide is ^{90}Zr, for which measurements of inelastic scattering of protons,[2] ^{3}He ions,[3] and ^{4}He ions[4,5] have recently been reported. ^{90}Zr has also received considerable theoretical treatment,[6] and the low-lying states have been described in terms of $g_{9/2}{}^2$ and $p_{1/2}g_{9/2}$ proton configurations. Recent support for the theoretical assignments has come from other experiments[7] as well as from the inelastic scattering experiments mentioned.

II. EXPERIMENTAL ARRANGEMENT AND PROCEDURE

The experiment was carried out in a 20-in. scattering chamber equipped with a remotely controllable arm on which was located a ΔE-E detector telescope. The chamber and its associated equipment has been described elsewhere.[8] The ΔE detector was a 500-μ surface-barrier silicon type and the E detector was a lithium-drift silicon unit of 2 mm thickness. The method of particle discrimination used here also is described in Ref. 8. It should be emphasized that in addition to selecting only tritons, the requirement of a coincidence signal from both the ΔE and E detectors substantially reduces unwanted events in the spectra. Also, reaction events occuring in the silicon itself usually are rejected because the mass-energy loss requirements are not met.

The arm on which the detector telescope was located could be precisely rotated around the target with accuracy of $\pm 0.1°$. The zero-degree point was estab-

† Work performed under the auspices of the U. S. Atomic Energy Commission.

[1] A preliminary account of the present work was given by E. R. Flynn, D. D. Armstrong, and A. G. Blair, Bull. Am. Phys. Soc. **11**, 752 (1966).

[2] W. S. Gray, R. A. Kenefick, J. J. Kraushaar, and G. R. Satchler, Phys. Rev. **142**, 735 (1966); **154**, 1206 (1967).

[3] E. F. Gibson, J. J. Kraushaar, B. W. Ridley, M. E. Rickey, and R. H. Bassel, Phys. Rev. **155**, 1208 (1967).

[4] C. R. Bingham, M. L. Halbert, and R. H. Bassel, Phys. Rev. **148**, 1174 (1966).

[5] E. J. Martens and A. M. Bernstein, Phys. Letters **24B**, 669 (1967).

[6] K. W. Ford, Phys. Rev. **98**, 1516 (1955); B. F. Bayman, A. S. Reiner, and R. K. Sheline, *ibid.* **115**, 1627 (1959); I. Talmi and I. Unna, Nucl. Phys. **19**, 225 (1960); V. K. Thankappan, Y. R. Waghmare, and S. P. Pandya, Progr. Theoret. Phys. (Kyoto) **26**, 22 (1961); S. Cohen, R. D. Lawson, M. H. Macfarlane, and M. Soga, Phys. Letters **10**, 195 (1964).

[7] D. L. Hendrie and G. W. Farwell, Phys. Letters **9**, 321 (1964); R. B. Day, A. G. Blair, and D. D. Armstrong, *ibid.* **9**, 327 (1964); J. L. Yntema, *ibid.* **11**, 140 (1964).

[8] A. G. Blair, Phys. Rev. **140**, B648 (1965).

lished with similar precision by performing left-right measurements of the elastic scattering cross section and adjusting the zero to produce equal results at equal left-right angles. The angular range of the detector arm was from 8° to 170°.

During all of the data runs, a monitor detector was used. This detector was a 500-μ silicon surface-barrier unit with sufficient gold absorber in front of it to stop the elastically scattered tritons within the detector volume. The output of this device served to indicate any severe changes in beam position or target characteristics, thus avoiding significant discrepancies in the angular distribution from such causes.

Standard electronics were used to amplify the detector signals and to establish the particle-mass gate which identified the tritons. The total energy pulses (the summed E and ΔE pulses) were then brought into a 1024-channel analyzer which served as an interface to an SDS-930 computer. The analyzer was gated on only when the double requirements of the desired particle mass and the ΔE-E coincidence were met. Additional information which was introduced into the computer was the monitor counts and the total beam charge. The latter was obtained from a digital current integrator which was connected to a Faraday cup in which the beam was stopped. The monitor counts consisted of pulses corresponding to elastically scattered tritons, with the selection being made by a single-channel analyzer at the entrance of the computer interface.

In the computer the data were stored in a 1024-word array in the magnetic-core memory. The computer is equipped with numerous interrupt features with various assigned levels of priority. In this instance, the energy data were given the highest level of priority so that all other input information or computer operations did not interfere with the pulse-height information. Introduced in succeeding order of priority was the information from the current integrator, from the monitor detector, and from the dead-time circuits. This latter information was provided by a signal from the pulse-height analyzer which appeared each time the analyzer had to reject a datum pulse because it was already occupied with the analysis of a previous pulse. All of this information was then accumulated in the proper locations in the computer memory. External command of the programmed system was available through the use of a typewriter console, so that the various modes of data handling could be performed by means of typed instructions. After a data-taking run was completed, the data contents of the computer memory were recorded on a magnetic tape for later data analysis and also listed on a fast printer for more immediate examination.

The computer program which controlled the data flow also contained, at a still lower priority level, provisions for obtaining least-squares fits to the peaks in the experimental spectra. These peaks were assumed to have the form of a skewed Gaussian with an exponential tail. The method of fitting this shape to the

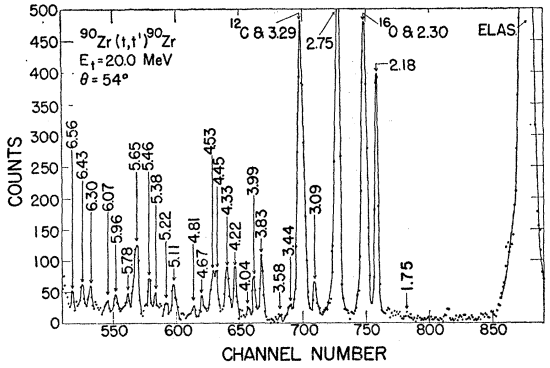

FIG. 1. Typical spectrum from the ^{90}Zr$(t,t')^{90}$Zr reaction. The solid curves represent the results of a least-squares fit to the data by means of a computer program which fits each peak with a skewed Gaussian distribution plus an exponential tail. The excitation energies are those determined in the present experiment. The 1.75-MeV-state excitation is particularly weak at this angle.

data has been described previously for off-line computers.[9] In the version of the peak-fitting program discussed here, it was possible to simultaneously fit two peaks and to obtain areas and locations for them. The areas were also divided by the current-integrator counts, multiplied by the dead-time correction factor and adjusted by some constant which could be typed in from the computer console. The results of the peak-fitting program were listed on the fast printer and put on the data magnetic tape. For a visual examination of the quality of the fit, a plotter was available which plotted both the data and the least-squares fit. All of this analysis was done while simultaneously recording data from the succeeding run. The parameters of the on-line fits were later used as first guesses in an off-line IBM 7094 program for data analysis of the peaks remaining to be analyzed.

All of the cross section and energy information to be discussed is the result of the least-squares analysis of the data, with the exception of the 1.75-MeV state, for which the peak areas were obtained by a simple sum. This state has a rather small cross section and there are special background problems related to the low-energy tail of the nearby elastic peak. This low-energy tailing is a characteristic problem of inelastic scattering studies and is primarily due to scattering of the incident beam from the defining slits of the scattering chamber.

Differential cross section measurements were carried out at angular intervals of 3° for most of the inelastic states to be discussed. The angular range for these states was from 18°–78° in the laboratory system. The elastic scattering cross section, however, was measured at angles as small as 12° and as large as 120°. Because of their greater intensity, the 2^+ and 3^- states at 2.18 and 2.75 MeV, respectively, were also measured out to 120°. Owing to the difficulty in extracting the weaker

[9] P. T. McWilliams, W. S. Hall, and H. E. Wegner, Rev. Sci. Instr. 33, 70 (1962); W. S. Hall (private communication).

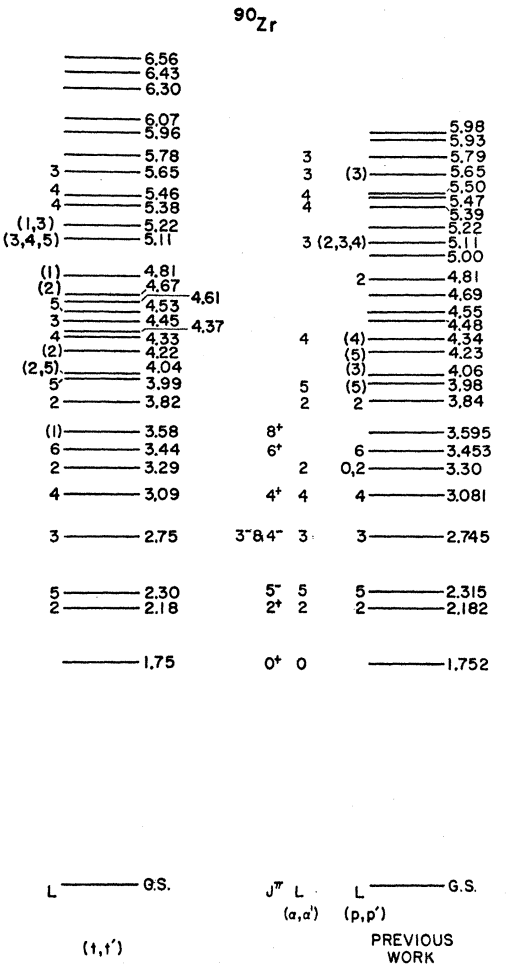

FIG. 2. Level diagram of present experimental results as compared to other experiments. Spins and parities are taken from Refs. 7 and 17, while L values from the $(\dot{p},\dot{p}')$ reaction come from Ref. 2 and those from the (α,α') reaction come from Ref. 5. For several states observed in the present experiment the analysis does not unambiguously determine the L value. For simplicity, only the assignments considered to be most probable are considered in the remaining figures and in the tables.

peaks from the low-energy tail of the elastic peak at small angles, data for these peaks are reported only for angles where they were clearly resolvable. The gain of the system was adjusted to about 18 keV/channel for the 1024-channel spectra in the computer. The lower-energy cutoff was determined by electronic gates and usually permitted a spectrum of about 7 MeV of excitation energy to be recorded. A typical energy spectrum is shown in Fig. 1 for an angle of 54°.

The energy resolution obtained during this experiment was about 60 keV, exclusive of the large-angle elastic scattering measurements for which the necessity of using reflection from the target resulted in poorer resolution. Over the energy interval considered, 30 states were observed. The energies of these states are shown in Fig. 2 where they are compared with previous data. These energies were assigned on the basis of an energy calibration provided by the position of the elastic peaks of ^{12}C and ^{16}O and were determined independently at several scattering angles. The error associated with the energies is ±15 keV up to 5.65 MeV, and ±25 keV above this value. Some of the observed states, however, were not of sufficient intensity to permit accurate angular distributions and these will not be discussed further. In particular, the levels above 5.65 MeV were not analyzed in detail.

TABLE I. Optical-model parameters used in all inelastic calculations.

V	152 MeV	a	0.684 F
W	19.6 MeV	b	0.771 F
r_s	1.24 F	r_c	1.25 F
r_i	1.48 F		

III. ANALYSIS

A. Elastic Scattering

Because of the similarity of the ^{3}He ion and the triton, one expects that triton elastic scattering can be described in a manner similar to the elastic scattering of ^{3}He ions. For some time, in fact, optical-model parameters for the triton for use in distorted-wave calculations, such as (d,t) reactions, have been inferred from ^{3}He-ion measurements. The optical-model analysis described below is based on previous results for ^{3}He-ion elastic scattering. A full report of this analysis, including results for several additional isotopes, has already been published.[10]

The optical potential employed for the triton has the following form:

$$U=-[V(r)+iW(r)]+V_c(r)$$
$$=-V\{1+\exp[(r-R_r)/a]\}^{-1}$$
$$-iW\{1+\exp[(r-R_i)/b]\}^{-1}+V_c(r), \quad (1)$$

where $R_x=r_xA^{1/3}$, and V_c is the Coulomb potential due to a uniformly charged sphere of radius $r_cA^{1/3}$. The values of the parameters in Eq. (1) are tabulated in Table I. These quantities were obtained by means of a least-squares-search computer program due to Perey[11] which adjusted those parameters which were preassigned as variables until the best fit to the data was obtained. The resulting description of the elastic scattering differential cross section is compared with the experimental data in Fig. 3. As discussed in Ref. 10, a large number of parameter families provide comparable fits to the data, but certain physical guidelines have been imposed to select the set shown. These are, namely, that r_r is held at approximately 1.25 F, the radius used in optical-model calculations for nucleon scattering, and that the real well depth is approximately three times that for the nucleon. These requirements are based on the assumption that because the binding energy of the

[10] J. C. Hafele, E. R. Flynn, and A. G. Blair, Phys. Rev. 155, 1238 (1967).
[11] F. G. Perey, Phys. Rev. 131, 745 (1963).

triton is small, the real-well parameters are approximately determined by the sum of the interactions of the individual nucleons with the scattering nucleus.

An interesting aspect of the triton elastic scattering potential is its detailed relation to that for the ^{3}He particle. Bassel *et al.*[12] have obtained a potential which simultaneously describes differential cross section data for both projectiles on a given target nucleus by introducing symmetry terms V and W. They find these terms to be

$$V(r)=V_A\left(1+\exp\frac{r-R_r}{a}\right)^{-1}\pm\left(\frac{N-Z}{A}\right)V_B,$$

$$W(r)=W_A\left(1+\exp\frac{r-R_i}{b}\right)^{-1}$$

$$\mp 4\left(\frac{N-Z}{A}\right)bW_B\frac{d}{dr}\left(1+\exp\frac{r-R_i}{b}\right)^{-1}, \quad (2)$$

where the upper sign refers to ^{3}He ions and the lower sign to tritons. In the recent analysis[10] of the ^{90}Zr-triton elastic scattering data, a smaller radius was obtained for the triton imaginary well than had been obtained previously for the ^{3}He-ion imaginary well. However, since it is to some extent the quantity Wr^n (where n is some constant) which is determined by the optical-model analysis, the results of the two analyses are somewhat equivalent. The important feature emerging from both analyses is that the imaginary (absorptive) term of the optical potential is of smaller magnitude for the triton than for the ^{3}He particle. Thus, somewhat less dominance of this term in the scattering process is expected for tritons. This point will be emphasized below in the discussion of inelastic scattering.

B. Inelastic Scattering

The data of the present experiment were analyzed by means of the distorted-wave (DW) approximation. The DW calculation has been employed successfully for several years in the interpretation of inelastic scattering results, although until recently, attention has been centered chiefly on the excitation of collective states.[13]

In the DW approximation the transition amplitude is given by

$$T_{if}=\int d\mathbf{r}\,\chi_f^{(-)*}(\mathbf{k}_f,\mathbf{r}_f)\langle\phi_f|v|\phi_i\rangle\chi_i^{(+)}(\mathbf{k}_i,\mathbf{r}_i). \quad (3)$$

The quantities $\chi(\mathbf{k},\mathbf{r})$ are the distorted waves which satisfy the Schrödinger equation for the elastic scattering potential for the entrance or the exit channel. These are obtained from the elastic scattering parameters given in Sec. III A. The usual procedure is to assume

[12] R. H. Bassel, R. M. Drisko, and P. G. Roos (private communication).

[13] R. H. Bassel, G. R. Satchler, R. M. Drisko, and E. Rost, Phys. Rev. 128, 2693 (1962).

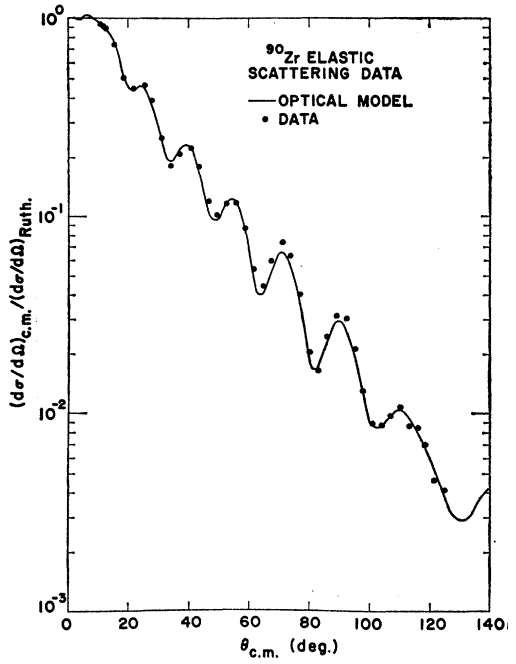

FIG. 3. Elastic scattering differential cross section divided by Rutherford cross section. The solid curve is the optical-model fit to the data. The statistical errors are smaller than the point size.

that the inelastic reaction is adiabatic, in which case the same potential is used in both channels. This is not always a satisfactory assumption, however. In some cases, for example, there is a strong dependence of the imaginary potential on the channel.[14] The remaining factor in Eq. (3), usually called the form factor, represents the transition between the two nuclear states designated by ϕ. The remaining discussion of this section will be concerned with two possibilities for this matrix element, namely, the collective-model form factors and the shell-model form factors. Through the present work the DW predictions result from the program JULIE.[15]

1. Collective Model

In this model the potential is assumed to be nonspherical with the interaction strength being determined by the deviation of the radius from the spherical surface. The details of the calculation have been described in Ref. 13 and only the results need be described here. The matrix element given for the interaction in Eq. (3) becomes

$$\langle\phi_f|v|\phi_i\rangle=\beta_L\left(R_r\frac{dV(r)}{dr}+iR_i\frac{dW(r)}{dr}\right)i^LY_L{}^M, \quad (4)$$

where $V(r)$ and $W(r)$ are as in relation (1) and β_L is the usual deformation parameter, which gives the strength

[14] E. R. Flynn and L. Rosen, Phys. Rev. 153, 1228 (1967).

[15] R. H. Bassel, R. M. Drisko, and G. R. Satchler, Oak Ridge National Laboratory Report No. ORNL-3240 (unpublished). We are indebted to Dr. Drisko for furnishing us with this program.

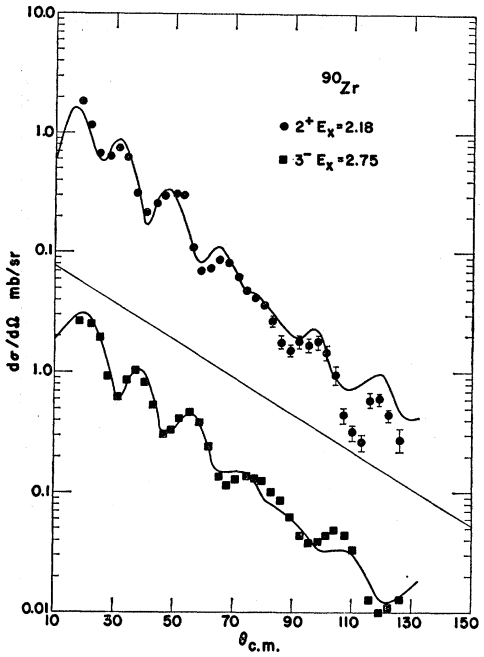

FIG. 4. Experimental angular distributions for the first 2^+ and 3^- states compared to the predictions from the DW calculation using a complex collective form factor. The prediction for the 2^+ state is corrected for Coulomb excitation.

of the interaction. The importance of deforming both the real and imaginary wells for ^{3}He particles has been previously pointed out[14,16]; without the imaginary term the values of β_L are far too large. Similar discrepancies might be expected to occur for the triton.

In Figs. 4 and 5, several experimental angular distributions are compared to predictions from the DW calculation using the collective form factor. The optical-model parameters in the calculation were taken from Table I. Figure 4 contains the known 2^+ state at 2.18 MeV and the known 3^- state at 2.75 MeV.[7,17] The 3^- state is usually regarded as an octopole one-phonon vibrational state, while the 2^+ state is usually described as a $g_{9/2}{}^2$ proton configuration, but is known to possess collective features as well. The values of β_L for these and some other states are given in Table II. The values of β_L for some of these same states were also determined in the (p,p') experiment,[2] the (^{3}He,^{3}He′) experiment of Gibson *et al.*,[3] and the (^{4}He,^{4}He′) experiment of Bingham *et al.*,[4] and are included in Table II. The agreement of the present results with the results from the (^{3}He,^{3}He′) and (^{4}He,^{4}He′) experiments is quite satisfactory. Comparison to the (p,p') results indicates good agreement for only the 2.18-MeV state, however, and the disagreement becomes particularly pronounced for the noncollective states. This result is not surprising,

[16] E. R. Flynn and R. H. Bassel, Phys. Rev. Letters **15**, 168 (1965).

[17] *Nuclear Data Sheets*, compiled by K. Way *et al.* (U. S. Government Printing Office, National Academy of Sciences–National Research Council, Washington, D. C., 1960), NCR 60-4-27.

TABLE II. Deformation parameters obtained from complex collective model.

E_x (MeV)	L	(p,p')[a]	(^{3}He,^{3}He′)[b]	(^{4}He,^{4}He′)[c]	(t,t')
2.18	2	0.07	0.073	0.058	0.070
2.30	5	0.075			0.039
2.75	3	0.16	0.11	0.120	0.12
3.09	4	0.04			0.027
3.29	2			0.035	0.040
3.44	6	0.09			0.016
3.82	2		0.047	0.043	0.047
3.99	5				0.027
4.04	5				0.022
4.22	2				0.037

[a] Values from Ref. 2.
[b] Values from Ref. 3.
[c] Values from Ref. 4.

since the β_L's extracted for noncollective states probably have little physical significance, but serve only to indicate their relative strengths. The results from the inelastic scattering of tritons, ^{3}He ions, and α particles tend to agree because these reactions are all strongly surface-peaked. In the case of the (p,p') reaction, on the other hand, the projectile samples more of the interior portion of the nuclear wave function, which, for noncollective states, can vary considerably from state to state.

In the discussion of elastic scattering it was noted that the imaginary radius for triton scattering was somewhat smaller than had been obtained for the ^{3}He particle (or alternatively, for the same radius the imaginary potential is shallower). From this observation it might be expected that for the triton scattering calculations, the imaginary part of the form factor as given by Eq. (4) might have somewhat less influence than it does in the case of the ^{3}He particle. This is indeed the case. Calculations where only the real part of Eq. (4) was included gave $\beta_2=0.12$ and $\beta_3=0.19$ for the 2.18- and 2.75-MeV states, respectively. This is an increase of slightly over a factor of $1\frac{1}{2}$ from the results given in Table II. For similar cases involving the ^{3}He particle, factors of two to three were obtained for β_L in passing from the complex form factor to the real form factor.[14,16]

The calculations for the 2^+ state at 2.18 MeV include a correction for Coulomb excitation of this state. The details of this correction are outlined in Ref. 13. The charge of the target nucleons was taken as equal to the electron charge; no effective charge which differed from this was tried. Addition of the Coulomb-excitation correction improved the theoretical fit to the data substantially, but had little effect on the value of β_L. The Coulomb-excitation correction is not included for states with angular momentum transfers greater than 2, since such corrections have little effect.[14]

Another effect which might possibly alter the angular distributions or the values of β_L is the use of an optical potential in the exit channel different from that in the entrance channel. It has been noted[14] in the inelastic scattering of ^{3}He ions from the highly collective first-

excited 2^+ states of ^{56}Fe, ^{58}Fe, and ^{58}Ni that a reduced value of W was required in the exit channel of the DW calculation to obtain the optimum fit to the data. A similar investigation for the 3^- collective states of those nuclei yielded inconclusive results. In the present situation, the 2^+ state at 2.18 MeV is not a strongly excited state in inelastic scattering, and one might expect that the importance of this effect would be less. Indeed, there is very little improvement in the DW fit when the value of W is altered in the exit channel over a range of ± 6 MeV from the normal value.

2. Shell Model

A shell-model analysis of inelastic scattering has been applied to a rather limited number of cases.[2,18–22] The most satisfactory results have, quite naturally, been obtained for nuclides in which the nucleon states may be assigned simple configurations. The target discussed here is excellent in this sense, since the outermost neutrons comprise a closed shell (the $g_{9/2}$ shell), and the proton ground-state configuration is known to be mainly a mixture of $p_{1/2}{}^2$ and $g_{9/2}{}^2$ proton configurations. The ground-state wave function thus has the form

$$|i\rangle = a|(\pi p_{1/2}{}^2)_0(\pi p_{3/2}{}^4)_0(\pi f_{5/2}{}^6)_0\cdots (\nu g_{9/2}{}^{10})_0(\nu p_{1/2}{}^2)_0\cdots\rangle + b|(\pi g_{9/2}{}^2)_0(\pi p_{3/2}{}^4)_0(\pi f_{5/2}{}^6)_0\cdots (\nu g_{9/2}{}^{10})_0(\nu p_{1/2}{}^2)_0\cdots\rangle, \quad (5)$$

where π refers to protons and ν refers to neutrons, and $a^2+b^2=1$. The wave function has been written in this way so as to indicate the shell-model orbitals which may be expected to contribute particles to low-lying excited states. The coefficients a and b have been measured,[7,23] and have also been calculated from theory.[6] The experimental values of a^2 range from 0.50 to 0.78, while the theoretical values fall between 0.64 and 0.75. The work of Ref. 2 assumed values of $a^2=0.64$ and $b^2=0.36$; we adopt these values in the present work. In addition, for the single-particle wave-function phase convention adopted here, theory predicts that the ratio b/a is positive.

The theory of inelastic scattering as described by a nuclear shell model has been presented in detail,[22,24] and will be only briefly outlined here. One supposes a two-body interaction between the incident projectile (in this case a triton) and each target nucleon, with the total effective interaction being the sum over all such interactions. The effective triton-nucleus interaction corresponding to the v of Eq. (4) is thus taken to be

$$v(\mathbf{r}_i,\mathbf{r}_t) = -\sum_i (V_0 + V_1 \boldsymbol{\sigma}_i\cdot\boldsymbol{\sigma}_t) g(|\mathbf{r}_i-\mathbf{r}_t|), \quad (6)$$

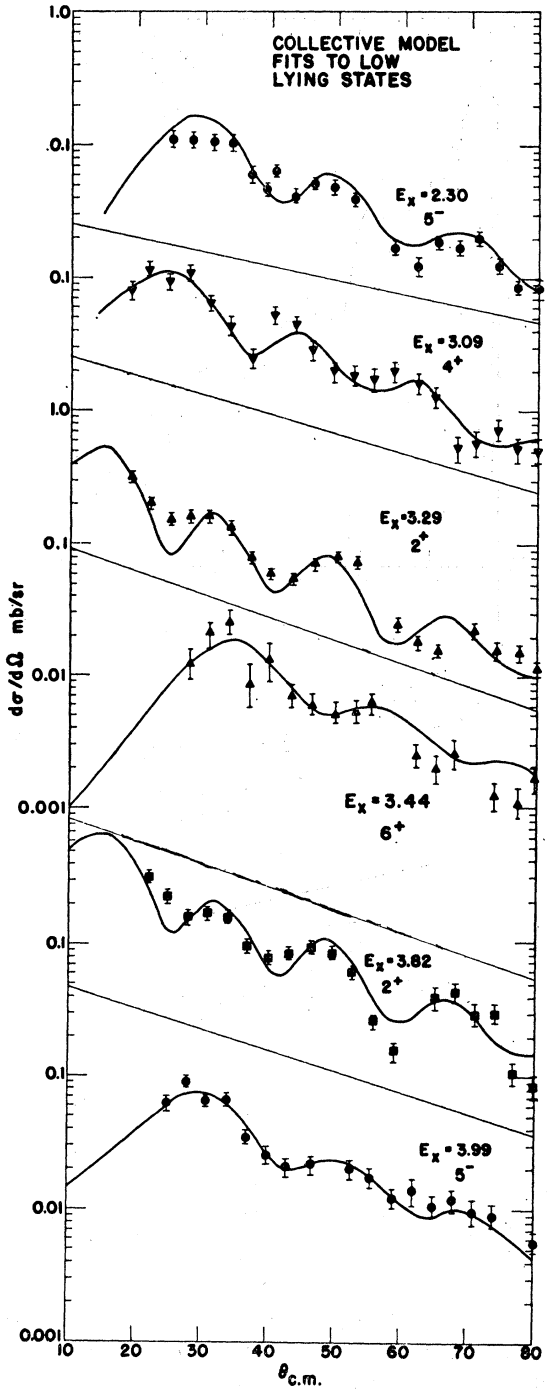

FIG. 5. Experimental angular distributions for several states compared to the predictions from the DW calculation using a complex collective form factor.

[18] M. B. Johnson, L. W. Owen, and G. R. Satchler, Phys. Rev. 142, 748 (1966); 154, 1206 (1967).
[19] G. R. Satchler, Nucl. Phys. A95, 1 (1967).
[20] M. M. Stautberg and J. J. Kraushaar, Phys. Rev. 151, 969 (1966).
[21] V. A. Madsen and W. Tobocman, Phys. Rev. 139, B864 (1965).
[22] N. K. Glendenning and M. Veneroni, Phys. Rev. 144, 839 (1966), and references therein.
[23] B. M. Preedom, Ph.D. thesis, University of Tennessee, 1967 (unpublished).
[24] G. R. Satchler, Nucl. Phys. 77, 481 (1966).

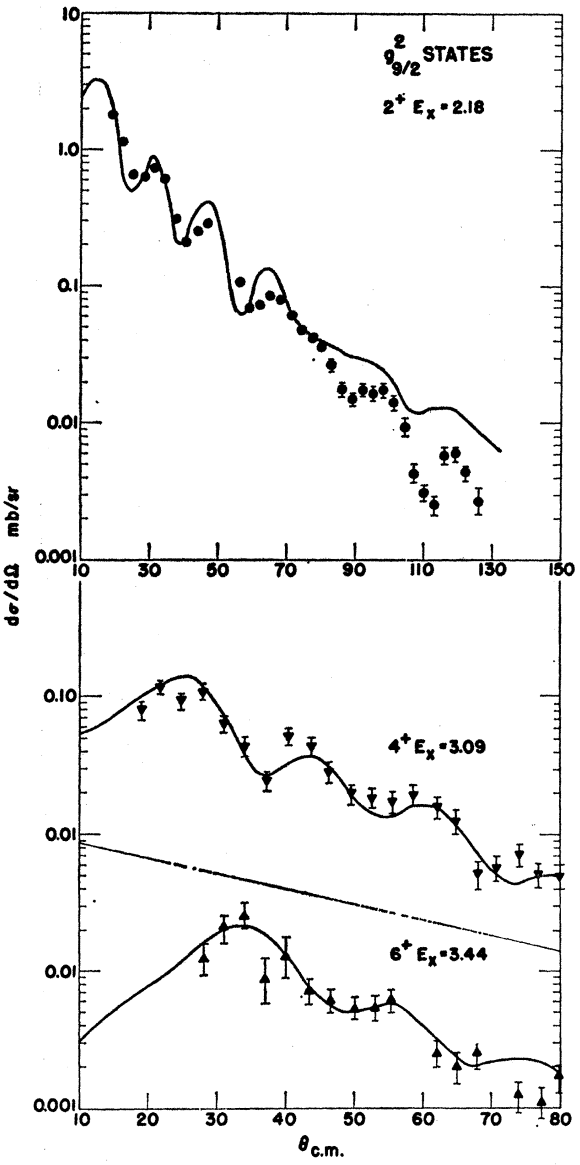

FIG. 6. Experimental angular distributions for the observed $g_{9/2}^2$ states compared to the predictions from the DW calculation using shell-model form factors. A Yukawa interaction with $\alpha = 1.0$ F^{-1} was used in the form-factor calculation.

where the subscripts i and t refer to a target nucleon and the triton, respectively, and the sum is over all target nucleons. The second term allows for spin-flip processes ($\Delta S = 1$) for the triton. The quantities V_s, where S is either 0 or 1, are also dependent upon the isospin and can be written

$$V_s = V_{s\alpha} + V_{s\beta} \tau_i \cdot \tau_t. \quad (7)$$

The radial dependence of the interaction is expressed in the $g(r_{it})$ term, where $r_{it} = |\mathbf{r}_i - \mathbf{r}_t|$. Several radial forms were investigated, including the Yukawa

$$g(r_{it}) = (\alpha r_{it})^{-1} \exp(-\alpha r_{it}), \quad (8)$$

the double Yukawa

$$g(r_{it}) = (\alpha r_{it})^{-1} \exp(-\alpha r_{it}) - C(\beta r_{it})^{-1} \exp(-\beta r_{it}), \quad (9)$$

and the Gaussian

$$g(r_{it}) = \exp(-\gamma r_{it}^2). \quad (10)$$

For a given choice of radial interactions, form factors were calculated by the use of the program ATHENA of Johnson and Owen.[25] The quantity calculated by this program is given by

$$I_L(r) = \int u_2(r_i) u_1(r_i) g_L(r_{it}) r_i^2 dr_i. \quad (11)$$

In Eq. (11), the u_i's are the wave functions for the single-particle configurations to be considered. The

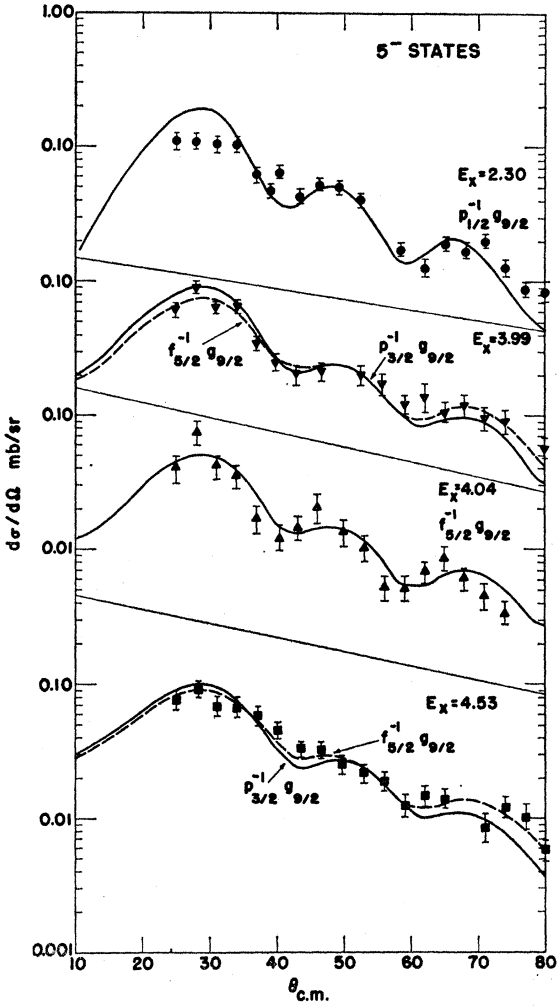

FIG. 7. Experimental angular distributions for the observed $L = 5$ transitions compared to the predictions from the DW calculation using shell-model form factors. A Yukawa interaction with $\alpha = 1.0$ F^{-1} was used in the form-factor calculation.

[25] M. B. Johnson and L. W. Owen (unpublished).

calculation assumes that u_i is a solution of a radial Schrödinger equation with a central potential given by the sum of a Woods-Saxon well, a Coulomb repulsion term, and a spin-orbit term. The potential parameters for the proton configurations were chosen to be identical to those used in the study of the ^{90}Zr(p,p') reaction.[18] For the neutron configurations employed, the well depths were chosen to give the experimental neutron-binding energies.[26] The form factors were found to be rather insensitive to a change of an MeV or so in binding energy. A nonlocality correction was also included, again identical to that used in the (p,p') study.

These form factors were then employed in the DW calculation, and the resulting quantities $\sigma_L(\theta)$ were compared to the experimental cross sections through the equation

$$d\sigma/d\Omega=(2J+1)(V_0^2M_L^2+V_1^2N_{LJ}^2)\sigma_L(\theta). \quad (12)$$

Equation (12) assumes that only a single value of L contributes. The reduced angular matrix elements M_L for $\Delta S=0$ and N_{LJ} for $\Delta S=1$ are defined in Ref. 18

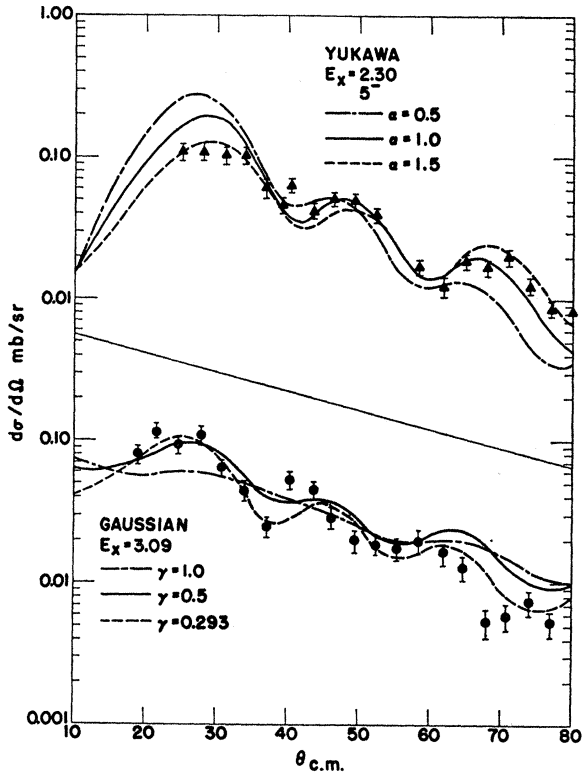

FIG. 8. The effect on DW predictions of varying the type and range of the radial interaction in the form-factor calculation. The upper part of the figure compares the data for the 5^- 2.30-MeV state to the predictions for a Yukawa interaction with different values of the range parameter α. The lower part of the figure compares the data for the 4^+ 3.09-MeV state to the predictions for a Gaussian interaction with different values of the range parameter γ. The values of $\gamma=0.293$ F^{-2} and $\alpha=1.0$ F^{-1} for the Gaussian interaction and the Yukawa interaction, respectively, correspond to the same range of interaction.

[26] B. L. Cohen, Phys. Rev. 130, 227 (1963).

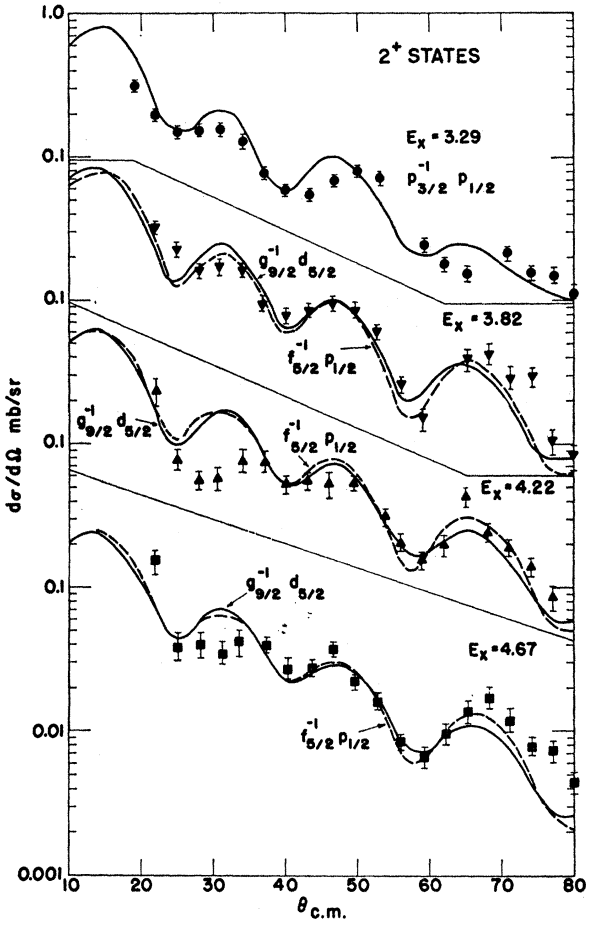

FIG. 9. Experimental angular distributions for all remaining $L=2$ transitions compared to the predictions from the DW calculation using shell-model form factors. A Yukawa interaction with $\alpha=1.0$ F^{-1} was used in the form-factor calculations for these transitions and for those in the remaining figures.

and tabulated in Ref. 2. In the present analysis we have neglected spin-orbit coupling in the distorted waves, and thus there is no predicted interference between $\Delta S=0$ and $\Delta S=1$ terms.

By comparing the DW predictions to the experimental distributions in those cases for which the configurations are known, one can, in principle, select the most nearly correct form of radial interaction and the best value of the range parameter α, β, or γ in Eqs. (8), (9), and (10). The strength of the interaction is given by the values of V_0 or V_1 required to produce the observed cross sections.

In the work which follows, the results of exciting certain states, whose configurations are regarded as well known, are compared to DW predictions employing form factors obtained for several values of the range parameters. It is established that, for these cases, the most satisfactory agreement is obtained for a Yukawa interaction potential with a range of about 1 F. This potential was therefore used to calculate form factors

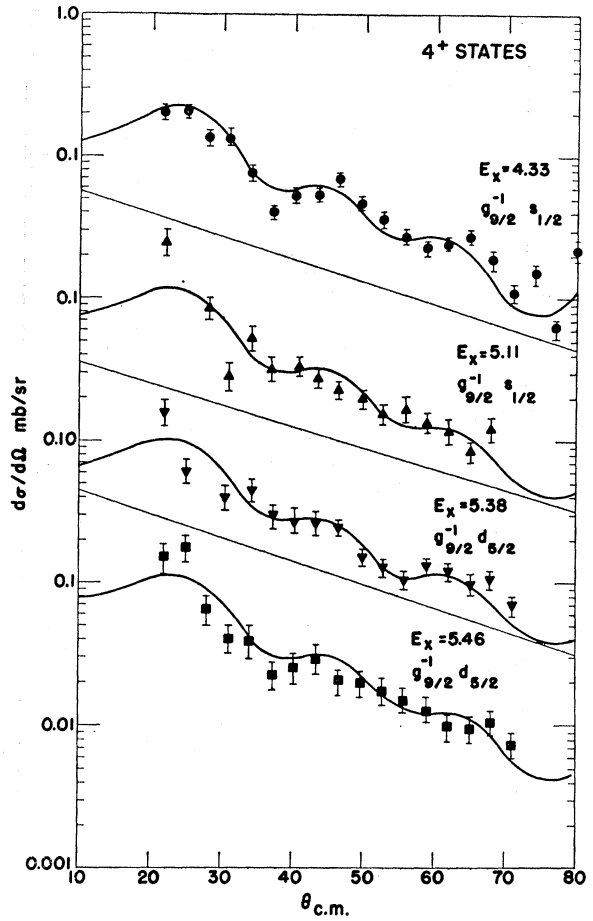

FIG. 10. Experimental angular distributions for all remaining $L=4$ transitions compared to the predictions from the DW calculation using shell-model form factors.

for various other configurations, and the resulting DW predictions were compared to the other observed distributions. Except for the 1.75-MeV 0^+ state, no mixed configurations for final states were considered. The comparisons for all states are shown in Figs. 6–12. It will be observed that, in general, the shape of a predicted angular distribution is sensitive chiefly to the transferred angular momentum, with relatively minor differences appearing from the use of the various configurations allowed.

The DW calculation used the optical-model parameter values given in Table I. The isospin-dependent potentials found by Bassel *et al.*,[12] and discussed in connection with Eq. (2), were tried for the case of the 3.09-MeV-state excitation; the predicted angular distribution was insensitive to this parameter change.

3. Shell-Model Comparison

The analysis of 19-MeV proton inelastic scattering on Zr isotopes yielded satisfactory agreement with the data when a Yukawa potential with a range parameter $\alpha \approx 1.0$ F^{-1} was used.[18–20] With this potential form, the strength was found to be $V_0 \approx 200$ MeV, $|V_1| \ll |V_0|$, and $|V_{0\beta}| \ll |V_{0\alpha}|$. It is not apparent *a priori* that the same interaction form should be used for triton scattering as for nucleon scattering, nor it it obvious what the interaction strength should be. The triton must be considered as a loosely bound system which can undergo considerable distortion in proximity to the target nucleus and does not penetrate deeply into the nuclear interior without breaking up. A proton or neutron projectile, on the other hand, penetrates more deeply into the nucleus and thus probes the nucleus differently

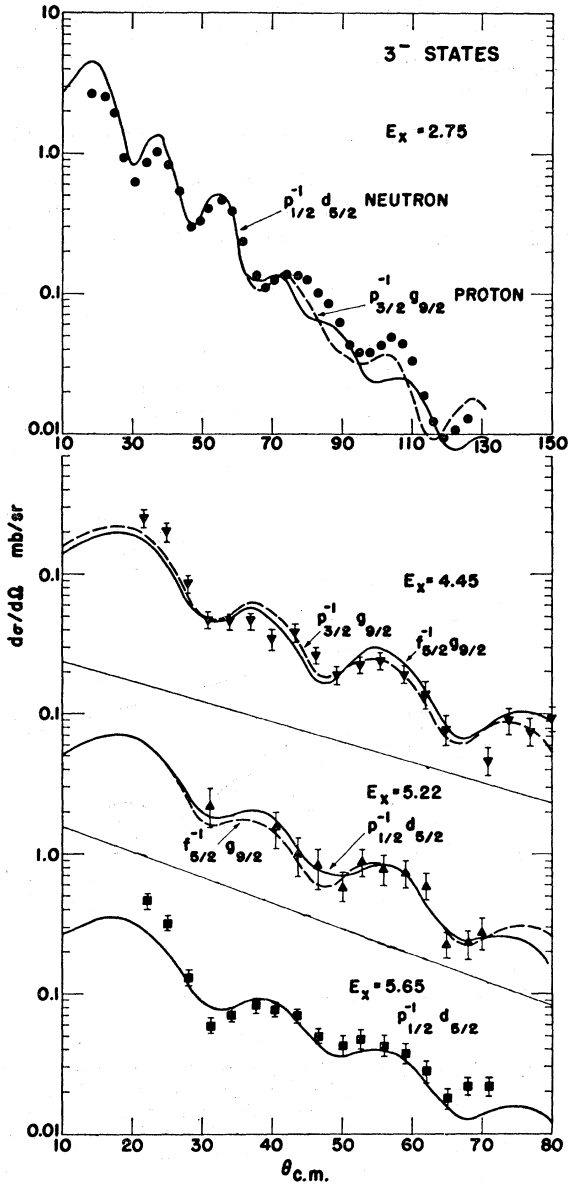

FIG. 11. Experimental angular distributions for all $L=3$ transitions compared to the predictions from the DW calculation using shell-model form factors. The $p_{1/2}^{-1}d_{5/2}$ configuration is for neutrons. Note the difference in the scale of the abscissa in the top part of the figure as compared to the bottom part.

than does a triton. However, by analogy to the argument used for the optical-model analysis, one might naively expect an interaction strength approximately three times that obtained from nucleon-nucleus scattering. It is interesting to note that Bingham *et al.*,[4] analyzing their data obtained by scattering 64-MeV ^{4}He particles from ^{92}Zr, obtained almost equally good fits to the distributions for the $d_{5/2}^2$ neutron states with a Gaussian or a Yukawa well, although the interaction strength showed some inconsistency between different states. They obtained a range parameter value of 0.5 F^{-1} for the Yukawa well and a corresponding effective strength of approximately 40 MeV.

The $g_{9/2}^2$ States. Some of the low-lying states of ^{90}Zr appear to be well described in terms of relatively pure $g_{9/2}^2$ and $p_{1/2}g_{9/2}$ proton configurations.[6,7] The $g_{9/2}^2$ configuration leads to 2^+, 4^+, 6^+, and 8^+ states, in addition to the 0^+ member which is split between the ground state and the 1.75-MeV state. The 2^+ member, at 2.18 MeV, is also expected to be somewhat collective in nature. The 4^+, 6^+, and 8^+ members of the configuration should describe the actual nuclear states fairly well, however, since there are no other simple low-lying configurations with these spins. Of the several radial dependences tried for the form factors for these states, only the Yukawa well, with a range of about 1.0 F, yielded satisfactory distributions. The results of using the other radial dependences will be discussed below in connection with the $p_{1/2}g_{9/2}$ 5^- state.

The data for the 2^+, 4^+, and 6^+ members of this configuration are compared with the predicted angular distributions in Fig. 6, while Table III lists the interaction strengths obtained. For the $g_{9/2}^2$ configuration, the nuclear matrix elements are functions of the amplitude b of Eq. (5), and the cross sections are thus functions of $V_0^2b^2$. There can be no contribution from the spin-flip term V_1 since such terms are forbidden for states belonging to the same j^n configuration as the ground state.[18] The potentials obtained for the 4^+ state at 3.09 MeV and the 6^+ state at 3.44 MeV are in good agreement with each other. The potential obtained for the 2^+ state is considerably higher, as expected if the state also has collective features. It is interesting to note that, in the present experiment, the value of V_0 obtained for this state is about 60% higher than for the 4^+ and 6^+ states, while in the (p,p') reaction study it was only 20% higher. From incoming momentum considerations, the $L=8$ component of the $g_{9/2}^2$ configuration should be quite weakly excited, and it was not observed in the present experiment. A state lying close to the expected position of the 8^+ state was observed (3.58 MeV), but its angular distribution revealed it to be a probable $L=1$ transition. (See the discussion later in the present section.) This identification could alleviate the difficulties with the unusual $L=8$ strength attributed to a state at this energy observed in the proton scattering experiment.[2]

The quality of the theoretical fit to the 2^+ state would probably improve if corrections for Coulomb-excitation effects were made. As noted in the discussion on the collective model, this correction, while improving the fit, does not substantially change the interaction strength. Another possible means of improving the comparison to the data is through the use of an asymmetric DW calculation, also discussed for the case of

TABLE III. Interaction strengths for excitation of various states in ^{90}Zr for assumed proton configurations.

E_x (MeV)	L	Assumed configuration	Strength (MeV) $a=0.8$, $b=0.6$
1.75	0	$a(g_{9/2}^2)-b(p_{1/2}^2)$	510
2.18	2	$g_{9/2}^2$	1230
2.30	5	$p_{1/2}g_{9/2}$	490
2.75	3	$p_{3/2}^{-1}g_{9/2}p_{1/2}^2$	1160
3.09	4	$g_{9/2}^2$	730
3.29	2	$p_{3/2}^{-1}p_{1/2}g_{9/2}^2$	700
3.44	6	$g_{9/2}^2$	770
3.58	1	$f_{5/2}^{-1}g_{9/2}p_{1/2}^2$	80
3.82	2	$f_{5/2}^{-1}p_{1/2}g_{9/2}^2$	860
3.99	5	$p_{3/2}^{-1}g_{9/2}p_{1/2}^2$	620
4.04	5	$f_{5/2}^{-1}g_{9/2}p_{1/2}^2$	640
4.45	3	$p_{3/2}^{-1}g_{9/2}p_{1/2}^2$	290
4.53	5	$f_{5/2}^{-1}g_{9/2}p_{1/2}^2$	660
5.22	3	$f_{5/2}^{-1}g_{9/2}p_{1/2}^2$	610
		$p_{3/2}^{-1}g_{9/2}p_{1/2}^2$	190
5.65	3	$f_{5/2}^{-1}g_{9/2}p_{1/2}^2$	1350
		$p_{3/2}^{-1}g_{9/2}p_{1/2}^2$	420

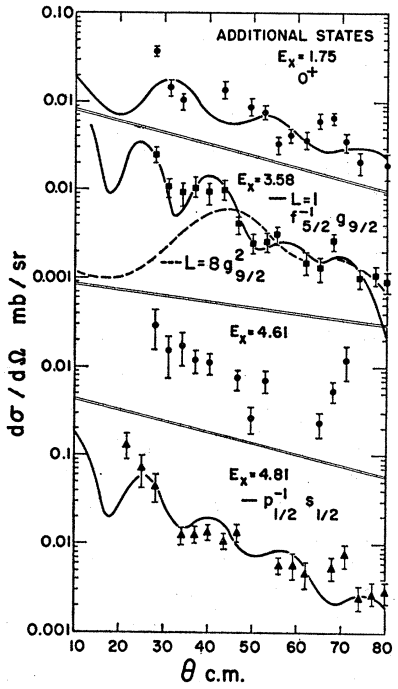

FIG. 12. Experimental angular distributions for several remaining states. The 1.75-, 3.58-, and 4.81-MeV-state distributions are compared to the predictions from the DW calculation using shell-model form factors. The distribution for the 3.58-MeV state is compared to predictions for both $L=1$ and $L=8$ transitions. The configurational assignment to the 4.81-MeV state assumes excitation via a spin-flip interaction.

TABLE IV. Comparison of strengths obtained for various forms and ranges of radial interaction.

Form	Range	Strength $g_{9/2}^2$ $L=4$ (3.09 MeV)	$g_{9/2}^2$ $L=6$ (3.44 MeV)	$p_{1/2}g_{9/2}$ $L=5$ (2.30 MeV)
Yukawa	$\alpha=0.5$ F^{-1}	64	115	62
	$\alpha=1.0$ F^{-1}	730	770	490
	$\alpha=1.5$ F^{-1}	3970	3200	2360
Gaussian	$\gamma=0.293$ F^{-2}	260	190	120
	$\gamma=0.5$ F^{-2}	980	670	420
Double Yukawa	$\alpha=1.0$ F^{-1} $\beta=1.1$ F^{-1} $C=1.0$	1970	2650	1420

the collective model. Since the results of Sec. III B 2 as well as those of Ref. 14 indicate that no appreciable change in strength would occur, no attempt to include either of these corrections was made. Indeed, because of the reduction in the effect of the imaginary potential on the cross sections compared with the case of the ^{3}He projectile, the results of an asymmetric DW calculation should be even less significant than for ^{3}He-particle scattering.

The $p_{1/2}g_{9/2}$ 5$^-$ State. The 4$^-$ member of the $p_{1/2}g_{9/2}$ proton configuration, at 2.75 MeV, can be excited only through a spin-flip interaction, but was not observed because of its near degeneracy with the collective 3$^-$ state. The 5$^-$ member, at 2.30 MeV, can be excited by both non-spin-flip and spin-flip interactions. Since this state contains components from both of the ground-state configurations, its excitation is dependent upon the values of both a and b in Eq. (5). Under the assumption that $a=0.8$ and $b=0.6$, the values of M_L and N_{LJ} in Eq. (12) become $M_5=0.287$ and $N_{55}=0.157$.[2] From the work of Ref. 2, there is evidence that in proton scattering the spin-flip strength V_1 is small compared with V_0, so that the second term in Eq. (6) could be neglected for this state. If this assumption is made in the present work, the comparison with the DW prediction (see Fig. 7) yields an interaction strength of 490 MeV. This value is about 35% below that obtained for the $g_{9/2}^2$ 4$^+$ and 6$^+$ states. If the term in V_1^2 is assumed to contribute significantly to the cross section, this would tend to lower the value of V_0 further. In the proton scattering experiment, the interaction strength obtained for this state was in agreement with that obtained for the $g_{9/2}^2$ 4$^+$ and 6$^+$ states, although the quality of fit to the experimental angular distribution was somewhat inferior.

In an attempt to explain the discrepancy observed for this state, several factors were investigated. Among these was the question of the proper radial interaction to be used in the form-factor calculation. To investigate this effect, calculations were performed with the three interaction forms, Eqs. (8), (9), and (10). Several values of range for each form were tried, both for the excitation of the 5$^-$ state and for the 4$^+$ and 6$^+$ members of the $g_{9/2}^2$ configuration. Figure 8 shows a few of the results of these calculations, and Table IV shows the strengths obtained for some of the cases examined.

In general, it was found that the Yukawa potential, with $\alpha=1$ F^{-1}, yielded those distributions which most closely represented the experimental angular distributions. All of the other potential forms that were tried produced distributions which for two or all three of the states either had incorrect slopes, incorrectly positioned peaks, the incorrect amount of structure, or combinations of these effects. For example, although the Yukawa potential with $\alpha=1.5$ F^{-1} yielded a fit to the $L=5$ distribution which is qualitatively as good as that obtained with $\alpha=1.0$ F^{-1} (see Fig. 8), the predicted distributions for $L=4$ and $L=6$ had insufficient structure, and the slope was not steep enough. As another example, for the $L=6$ case the double Yukawa well with $\alpha=1.0$, $\beta=1.1$, and $C=1.0$, yielded a distribution very similar to the one obtained for the single Yukawa well with $\alpha=1.0$, but for the $L=4$ and $L=5$ cases the slope was too steep. Going to $\alpha=0.5$, $\beta=1.0$, and $C=2.0$ yielded distributions in which the slopes were even steeper.

Thus, we conclude that of the various radial-interaction forms tried, the Yukawa well with $\alpha=1.0$ F^{-1} yields angular distributions which best represent the data. All of the remaining calculations were performed with a Yukawa well of this range. No attempt was made to investigate the effect of changing the nonlocality range in the form-factor calculation.

Since the excitation of the $p_{1/2}g_{9/2}$ configuration depends upon the values of both a and b in Eq. (5), while the excitation of the $g_{9/2}^2$ configuration depends only upon b, one can consider what effect would be produced by choosing somewhat different values for these amplitudes. Using $a\approx b\approx 0.7$, one finds that V_0 is raised to 510 MeV for the 2.30-MeV state and lowered to 630 and 660 MeV for the 3.09-MeV and 3.44-MeV states, respectively. Although the discrepancy between the strengths for the excitation of the two configurations is thus reduced to an acceptable 20%, this choice for the values of a and b is rather on the limit of the range determined by previous experiments.[7,23]

It is possible that the states under discussion, particularly those of the $g_{9/2}^2$ configuration, are not as pure as has been presumed. It has already been shown that the 2$^+$ member of this configuration exhibits collective features, and we have remarked that, in the present experiment, the interaction strength obtained for the excitation of this 2$^+$ state is considerably larger, relative to the strengths obtained for the other $g_{9/2}^2$ states, than it is in the (p,p') experiment. For this 2$^+$ state, the difference between the results from the two experiments is probably due mainly to the fact that the wave function of the state is not well described by a simple $g_{9/2}^2$ configuration but contains several other configurations as well. The proton and triton projectiles are sensitive to somewhat different regions of the nuclear form factor, and the use of an incorrect form factor in the analyses of the data may lead to different

(incorrect) results in the two experiments. It is possible that there is also sufficient mixing of other configurations in the 4^+ and 6^+ states to yield somewhat different results in the two experiments.

Other Configurations. In addition to the $g_{9/2}^2$ and $p_{1/2}g_{9/2}$ configurations just discussed, other proton configurations should occur at relatively low excitation energies from the promotion of $2p_{3/2}$ and $1f_{5/2}$ protons to the unfilled $2p_{1/2}$ or $1g_{9/2}$ orbitals. At somewhat-higher energies (beginning at approximately 6 MeV), configurations will occur due to the excitation of $1f_{7/2}$ protons to these two unfilled orbitals, and also by the promotion of $p_{1/2}$ and $g_{9/2}$ protons to the $2d_{5/2}$ orbital. Figure 13 shows the approximate energy locations of these shell-model orbitals in the ^{90}Zr nucleus. If spin-flip possibilities are neglected, the angular momentum states available from the lower proton configurations are as follows: $p_{3/2}^{-1}p_{1/2}$, $L=2$; $p_{3/2}^{-1}g_{9/2}$, $L=3,5$; $f_{5/2}^{-1}p_{1/2}$, $L=2$; and $f_{5/2}^{-1}g_{9/2}$, $L=3,5,7$. In addition, one expects to excite configurations obtained by promoting a *neutron* from the filled $1g_{9/2}$ and $2p_{1/2}$ orbitals to the $2d_{5/2}$ and $3s_{1/2}$ orbitals; these configurations should not appear at energies lower than approximately 4 MeV. Some of these configurations, i.e., the $p_{3/2}^{-1}g_{9/2}$ and $f_{5/2}^{-1}g_{9/2}$ proton configurations and the neutron configurations, can couple to either $(p_{1/2}^2)_0$ or $(g_{9/2}^2)_0$ protons or to linear combinations of the two. Thus, from the excitation of the low-lying proton configurations just considered, one expects to observe two $L=2$, four $L=3$, and four $L=5$ transitions, and from the neutron configurations two $L=1$, two $L=2$, four $L=4$, and two $L=6$ transitions. (Only $\Delta T=0$ transitions are considered.) Of course, in the actual nuclear states these configurations will be mixed with each other and with still other configurations. Thus, it is not possible to assign them to the various observed states with any degree of authority. However, it is instructive to make representative assignments somewhat in the expected order of appearance, in order to get an idea of the magnitude of the interaction strength required for the various configurations. These assignments and the resulting strengths are shown in Tables III and V. Most of the strengths in Table III (which lists only proton-configuration assignments) are remarkably similar to the strengths obtained for the 4^+ and 6^+ members of the $g_{9/2}^2$ proton configuration and the 5^- member of the $p_{1/2}g_{9/2}$ proton configuration. The strengths shown in Table V (neutron configurations) on the other hand, are considerably lower. We now discuss the results shown in these two tables in more detail.

At energies above that of the 2.18-MeV 2^+ state already discussed, the next two states, for which the present experiment yields $L=2$ transitions, appear at 3.29 and 3.82 MeV. Their distributions are shown in Fig. 9. On the assumption that these states are pure $p_{3/2}^{-1}p_{1/2}$ and $f_{5/2}^{-1}p_{1/2}$ proton configurations, respectively, the extracted strengths are in fairly good agreement with the expected strengths. Two additional states

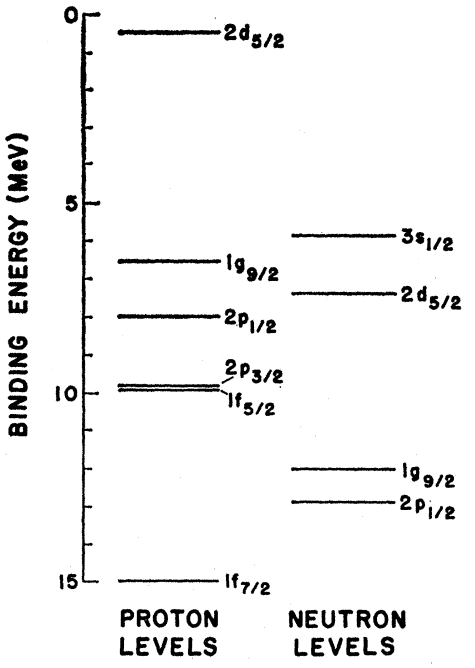

FIG. 13. Approximate energies of shell-model orbitals in the ^{90}Zr nucleus. Relative energies of proton levels are taken from calculations by S. Fallieros, quoted by D. Drechsel, J. B. Seaborn, and W. Greiner, Nucl. Phys. A94, 698 (1967). The absolute scale for the proton levels is based on the observed binding energy of the $p_{3/2}$ state (Ref. 23). Energies of neutron levels are taken from Ref. 26.

with probable $L=2$ transitions lie at 4.22 and 4.67 MeV, and are compared in Fig. 9 with the predictions for the $g_{9/2}^{-1}d_{5/2}$ neutron configuration. The quality of fit, particularly for the 4.22-MeV state, is poor in the forward-angle region, and the $L=2$ assignment to these states is therefore less certain than it is for the other $L=2$ states.

Table V shows the strength obtained for the excitation of the 4.22- and 4.67-MeV states under the assignment of a $g_{9/2}^{-1}d_{5/2}$ neutron configuration coupled to $(p_{1/2}^2)_0$ protons. The low strengths obtained suggest that this assignment is inadequate for either of the two states. However, another possible effect, the isospin dependence of the triton-nucleon interaction, must be kept in mind. Since the isospin of the triton, τ_t, is the same as that of a neutron, the product $\tau_i \cdot \tau_t$ in Eq. (7) will be positive if a neutron is being excited, and negative if a proton is being excited, just the opposite of the situation for proton inelastic scattering. If $V_{0\beta}$ had a magnitude which was an appreciable fraction of the magnitude of $V_{0\alpha}$, but had a negative sign (as in a Serber exchange mixture for nucleon-nucleon scattering), the result would be a lower effective V_0 for the excitation of neutron states than for the excitation of proton states. However, if the isospin-dependent interaction were important in triton scattering, one might also expect to see its effect in proton scattering. As mentioned earlier, proton inelastic scattering measure-

TABLE V. Interaction strengths for excitation of various states in ^{90}Zr for assumed neutron configurations, with protons in $(p_{1/2}^2)_0$ configuration.

E_x (MeV)	L	Assumed configuration	Strength (MeV) ($a=0.8$, $b=0.6$)
4.22	2	$g_{9/2}^{-1}d_{5/2}$	220
4.33	4	$g_{9/2}^{-1}d_{5/2}$	350
4.67	2	$g_{9/2}^{-1}d_{5/2}$	150
4.81	1	$p_{1/2}^{-1}s_{1/2}$	150
5.11	4	$g_{9/2}^{-1}s_{1/2}$	260
5.38	4	$g_{9/2}^{-1}d_{5/2}$	260
5.46	4	$g_{9/2}^{-1}d_{5/2}$	280

ments on ^{92}Zr, for which the lowest-lying states can be identified as due to the excitation of the $d_{5/2}^2$ neutron configuration, suggest that $|V_{0\beta}| \ll |V_{0\alpha}|$ for proton-nucleon interaction.[20]

An interesting comparison between the data of the present experiment and those of the (p,p') experiment can be made concerning the two $L=2$ states at 3.82 and 4.67 MeV. The (p,p') reaction identified two strong $L=2$ transitions at 3.84 and 4.69 MeV, and the cross sections of the two distributions were essentially identical. In the present experiment, the 3.82-MeV state is excited with between two and three times the intensity of the 4.67-MeV state. There are two apparent explanations for the different results from the two experiments. The first explanation returns to the possibility of a significant isospin dependence in the interaction, as discussed above. If the two states are predominantly proton configurations and neutron configurations, respectively, and if $|V_{0\beta}|$ is an appreciable fraction of $|V_{0\alpha}|$, the ratio of the cross sections for the two states would be different in the two experiments. An alternative explanation can be given in terms of the shapes of the form factors for the two states. If the form factor for the 3.82-MeV state extends to larger radii than does the form factor for the 4.69-MeV state, then triton inelastic scattering, which is relatively sensitive to the form factor at the nuclear surface and beyond, would excite the former state relatively more strongly than would proton inelastic scattering. An example of this effect appears in the calculation for the excitation of 5^- configurations. For the (p,p') reaction, the cross section predicted for the excitation of the $(p_{3/2}^{-1}g_{9/2})_5$ configuration is smaller than that predicted for the $(f_{5/2}^{-1}g_{9/2})_5$ configuration (see Fig. 9 of Ref. 2), but the former configuration is predicted to be excited twice as strongly as the latter in the (t,t') reaction.

Besides the $L=4$ transition to the known 4^+ state at 3.09 MeV, there are four other probable $L=4$ transitions observed in the present experiment, in agreement with the expected number of low-lying neutron configurations. The experimentally observed angular distributions are compared in Fig. 10 to the DW predictions using the $(\nu g_{9/2}^{-1}d_{5/2})_4(\pi p_{1/2}^2)_0$ and $(\nu g_{9/2}^{-1}s_{1/2})_4$-$(\pi p_{1/2}^2)_0$ configurations, and the resulting strengths are shown in Table V. The configuration assignments are, of course, only illustrative, but show that for these states the assumption of pure neutron configuration again yields interaction strengths considerably smaller than those obtained for the $g_{9/2}^2$ proton states. There is some question about the assignment of $L=4$ to the 5.11-MeV distribution. In our opinion, the distribution is best represented by the $L=4$ prediction, but an $L=3$ or $L=5$ assignment cannot be excluded.

A large number of experimentally observed states correspond to odd-L momentum transfers. Under the continued assumption that the spin-dependent potential V_1 in Eq. (6) is small, these states have spins and parities 1^-, 3^-, and 5^-. Figure 7 shows the $L=5$ angular distributions that were observed. The state at 2.30 MeV has already been discussed in terms of the $p_{1/2}^{-1}g_{9/2}$ proton configuration. Of the four anticipated additional $L=5$ configurations, three are identified, and are compared in Fig. 7 with predictions from the DW calculation. Of these distributions, the relatively poor statistics for the 4.04-MeV state would also permit an $L=2$ assignment, although with reduced probability. The comparison of the predictions for the $p_{3/2}^{-1}g_{9/2}$ and the $f_{5/2}^{-1}g_{9/2}$ configurations in Fig. 7 illustrates the insensitivity of the DW calculation to the form factor used, as regards the shape of the predicted distribution. The interaction strengths depend sensitively on the choice of configurations; for the assignments of Table III the strengths are similar to those obtained for the previously discussed proton states. Using the $p_{3/2}^{-1}g_{9/2}p_{1/2}^2$ configuration for the states at 4.45 and 4.53 MeV would result in considerably lower interaction strengths, however.

Figure 10 shows the distributions obtained which correspond to $L=3$ transitions. Owing to the relatively poor statistics and the lack of forward-angle points, the 5.22-MeV distribution could also be assigned to an $L=1$ transition, with somewhat reduced probability. The expected low-lying configurations for 3^- states were listed earlier; however, the collective state at 2.75 MeV should be a superposition of these and other particle-hole configurations. The present results are in agreement with this statement; when the distribution for the 2.75-MeV state is compared with the prediction for the pure $p_{3/2}^{-1}g_{9/2}p_{1/2}^2$ proton configuration, a strength of 1160 MeV is obtained. The assumption of an $f_{5/2}^{-1}g_{9/2}$ proton configuration would yield a considerably higher strength. Also, the shell-model form factor yields a predicted angular distribution which is not in as good agreement with the experimental points as that obtained with the collective form factor (see Fig. 4).

The interaction strengths for the excitation of $L=3$ states are also very sensitive to the proton configurations assumed, as shown in Table III for the 5.22- and 5.65-MeV states. There is a tendency, however, toward a low value of interaction strength for the 4.45-MeV state and the 5.22-MeV state. The cross section for the 5.65-MeV state is considerably larger than that for the

two lower $L=3$ states, as reflected in the results of Table III. The 3^- states are probably substantially mixed by collective forces, and single configurational assignments are especially inappropriate for them.

Two states with probable $L=1$ distributions were observed in the present experiment, and are shown in Fig. 12. The weakly excited state at 3.58 MeV is at the approximate location of the 8^+ state observed in other experiments,[17] but comparison to the DW predictions for a $g_{9/2}^2$ configuration shows that this assignment disagrees with the present measurements. Indeed, the strength required to produce the observed fit is considerably larger than that required for the other $g_{9/2}^2$ states. However, as seen in the figure, the distribution is quite well reproduced by the prediction for an $L=1$ transfer. There is no expected 1^- configuration in this energy region. However, the 2^- member of the $f_{5/2}^{-1}g_{9/2}$ proton configuration could be excited by means of an $L=1$, $\Delta S=1$ transfer. The effective interaction strength required for this situation is $V_1\approx 80$ MeV, or a little more than 10% of the strength obtained for the $g_{9/2}^2$ states. The other possible assignment to this state is the neutron configuration $p_{1/2}^{-1}s_{1/2}$, but since this configuration should appear at a higher energy it is perhaps more reasonable to assign it to the other $L=1$ state, at 4.81 MeV. This assignment, $(\nu p_{1/2}^{-1}s_{1/2})_1(\pi p_{1/2}^2)_0$, yields an interaction strength of 150 MeV, as shown in Table V.

The distribution for a peak observed at 4.61 MeV is also shown in Fig. 12, but no single value of angular momentum transfer could be assigned to it. The peak probably represents a mixture of two or more weak states.

The final state to be discussed is the 1.75-MeV 0^+ state. This state is believed to have a wave function which is the complement of the ground-state wave function.[6] The transition amplitude is proportional to the product ab times the difference between the radial form factors.[18] Calculations for the (p,p') experiment of Ref. 2 differed from the experimental distribution by an order of magnitude, although only a few data points were available. The (p,p') reaction has since been investigated at a beam energy of 12.7 MeV;[19,27] again, the 1.75-MeV state remains an order of magnitude smaller than that predicted.

In the present experiment, the data for this state are also rather poor because of the elastic tailing contribution, but are adequate to obtain points with errors of $\pm 20\%$. Figure 12 compares the theoretical calculation with the experimental data. Although the fit is poor, the calculation reproduces the rather flat nature of the distribution. The effective strength obtained is 510 MeV, about 25% lower than was obtained for the average of the $p_{1/2}^{-1}g_{9/2}$ 5^- state and the $g_{9/2}^2$ 4^+ and 6^+ states. In view of the experimental uncertainties, the results are satisfactory, and are in marked contrast to the poor agreement obtained in the (p,p') experiments.

The reason for the better agreement for this state in the present experiment may be related to the fact that the form factor for this configuration is particularly large near the center of the nucleus, and consequently particularly small in the nuclear surface. Johnson *et al.*[18] have suggested that the nuclear interior may be playing an exaggerated role in the DW calculation for the (p,p') excitation of this particular state. In the present work, the strong absorption of the triton effectively reduces the contribution from the interior of the nucleus in the DW calculation, and thus yields a smaller cross section for the (t,t') reaction.

IV. SUMMARY

The present results indicate that studies of the (t,t') reaction provide useful spectroscopic information. Subject to the usual conditions that the data extend over a sufficiently large angular range, and that the states are adequately resolved and are not too weakly excited, the comparison of the experimental angular distributions with DW predictions usually permits unambiguous L assignments. Many of the states in the present experiment were weakly excited or poorly resolved, of course, and for them the assignments are necessarily less certain. At higher excitation energies, the distributions tend to have less structure, particularly for the higher L values, and for these states the degree of confidence of the L assignments is somewhat lower. The (t,t') angular distributions tend to show somewhat more structure than do the (p,p') angular distributions at approximately the same bombarding energy, however, particularly for the higher angular-momentum transfers. For this reason, the identification of L values may be somewhat easier to make in studies of (t,t') reactions than in studies of (p,p') reactions. The structure of the angular distributions from the present experiment is not so pronounced as it is for 31-MeV ^{4}He-ion scattering,[5] however.

The present analysis has shown that the shapes of the predicted angular distributions are determined primarily by the angular momentum transfer, and are relatively insensitive to the form factors used, whether collective or one of several choices of shell-model configurations.

The agreement between the present assignments of L values and the results of previous experiments is good. For those assignments considered fairly definite in both the present experiment and previous experiments, there is apparent disagreement for only the state at 3.58 MeV. As discussed earlier, this disagreement is probably due to the occurrence of a doublet at this energy.

One of the interesting results of the elastic scattering analysis and the collective-model DW analysis is the reduced effect of the absorptive potential as compared to measurements with ^{3}He projectiles. The different

[27] J. K. Dickens, E. Eichler, R. J. Silva, and G. Chilosi, Oak Ridge National Laboratory Report No. ORNL-3934 (unpublished).

isospin of the two projectiles is evidently playing a strong role in the interaction. If this isospin dependence can be well described, studies involving the two projectiles should give useful information about isospin properties of nuclei.

The analysis of several distributions in terms of the collective-model DW calculation yielded deformation parameters in good agreement with those obtained in (^{3}He,^{3}He′) and (^{4}He,^{4}He′) experiments, but in poor agreement, in general, with the results of the (p,p') experiment.

When the DW calculation employing shell-model form factors was applied to those states usually described as single-configuration states, the use of a Yukawa interaction potential with a range of 1.0 F yielded predicted angular distributions in good agreement with the data. This was also the most suitable potential form found in the analysis of the ^{90}Zr(p,p') reaction study.[18] Under the assumption that the ^{90}Zr ground-state wave function can be described as a mixture of $p_{1/2}{}^2$ and $g_{9/2}{}^2$ proton configurations in the amplitude ratio of 0.8 and 0.6, respectively, an interaction strength of 660 MeV was obtained as an average for the states at 2.30, 3.09, and 3.44 MeV. This value of 660 MeV can be compared to the value of 200 MeV obtained for the excitation of these same states in the ^{90}Zr(p,p') reaction study. The experimental evidence thus indicates that, within the framework of the interaction model being used, the effective interaction strength is about three times as high for triton projectiles as for proton projectiles. This result is support of the frequently expressed belief that the optical potential for the three-nucleon projectile (^{3}He particle or triton) should be approximately three times that for a nucleon (see Sec. III A). Recent theoretical calculations are in agreement with this assumption.[28]

Representative interaction strengths were obtained for the other observed states by arbitrarily assigning pure configurations based on approximate energies of unperturbed shell-model orbitals. In spite of the necessarily unsatisfactory and incomplete nature of this approach, it is a rather striking fact that most of the resulting strengths for those states assigned to proton configurations are of the same order of magnitude, centered about the 660-MeV value obtained above, while all of the states assigned to neutron configurations have strengths considerably below this value. The most likely reason that these latter strengths are so low is that the assumed configurations for these states, all of which lie above 4 MeV of excitation, are actually considerably split over many states; i.e., the pure configuration assignments are grossly invalid. An alternative explanation, that $V_{0\beta}$ in Eq. (7) is large, seems less likely, since the results of the (p,p') reaction on the $d_{5/2}{}^2$ neutron states in ^{92}Zr are consistent with $|V_{0\beta}| \ll |V_{0\alpha}|$.[20] The ^{92}Zr($t,t'$) reaction is presently under study at this laboratory, and the results should help clarify the situation for triton scattering. It would also be of interest to reinvestigate the ^{90}Zr(^{3}He,^{3}He′) reaction[3] with somewhat better energy resolution, and to perform a shell-model analysis of the results, since for the (^{3}He,^{3}He′) reaction the interaction term $V_{0\beta}\boldsymbol{\tau}_i\cdot\boldsymbol{\tau}_t$ would have a sign opposite to that for triton scattering.

There is no indication from the present work that the spin-flip interaction potential V_1 is large for triton scattering. On the contrary, there is weak evidence (see the discussion for the 2.30- and 3.58-MeV states) that the value of V_1 is small, perhaps on the order of 10% of V_0. All of the states except the one at 3.58 MeV were analyzed under the assumption that $V_1 \approx 0$.

The major discrepancies between the present results and those from the (p,p') reaction study concern the excitation of the states at 1.75, 2.30, and 3.58 MeV. In the present experiment, the interaction strength for excitation of the 1.75-MeV 0^+ state is within 25% of the expected value, while in the (p,p') study it was too low by a factor of three. On the other hand, the (p,p') study yielded an interaction strength for the excitation of the $p_{1/2}g_{9/2}$ 5^- state at 2.30 MeV which agreed with that obtained for the $g_{9/2}{}^2$ 4^+ and 6^+ states, while in the present study the strength for the excitation of the former state is somewhat reduced. Finally, the present experiment indicates that the state excited at 3.58 MeV, at the approximate position of the 8^+ member of the $g_{9/2}{}^2$ configuration, corresponds to an $L=1$ transition, and thus the 8^+ state is probably excited too weakly to be observed.

The fact that the triton interacts more strongly at the nuclear surface than does the proton apparently produces some of the differences noted between the results from the present experiment and those from the (p,p') experiment. It is to be hoped that such differences can eventually provide detailed information bearing on nuclear wave functions.

ACKNOWLEDGMENTS

We wish to thank G. R. Satchler of the Oak Ridge National Laboratory for his many comments on this work and for supplying us with the code ATHENA. We are indebted to R. Woods and the crew of the tandem for furnishing the excellent triton beam. We also wish to thank W. S. Hall and J. Levin for providing the on-line computer program.

[28] A. Y. Abul-Magd and M. El-Nadi, Progr. Theoret. Phys. (Kyoto) 35, 798 (1966).